Electronic surface states on (111) aluminum*

Ed Caruthers, Leonard Kleinman, and Gerald P. Alldredge
Department of Physics, University of Texas, Austin, Texas 78712
(Received 23 October 1973)

We have calculated the projection of the three-dimensional energy bands of aluminum onto the two-dimensional Brillouin zone (BZ) of the (111) face. Using a pseudopotential constructed in the same way as that in our publications on the (001) and (110) faces, we have calculated eigenvalues and eigenfunctions at high-symmetry points of the two-dimensional BZ for (111) thin films. Unlike Boudreaux who found surface states only in the gap around $\bar{\Gamma}$, we find surface states exist in all the energy gaps of the projected bands at the $\bar{\Gamma}$, $\bar{M}$, and $\bar{K}$ symmetry points of the two-dimensional BZ. We conjecture that surface states always exist in the projected energy gaps of low-index surfaces of simple metals. For the first time we find a surface eigenfunction which decays inwardly from one surface toward the other; heretofore all surface states we have found decay inwardly from both surfaces toward the center of the film.

In this paper we apply to the (111) face of aluminum our method of projecting the two-dimensional energy bands which we have previously applied to the (001)[1] and (110)[2] faces of aluminum. This projection shows band gaps throughout most of the two-dimensional Brillouin zone (2D BZ) in which surface states could occur. Some of the gaps lie above the Fermi surface, but most occur in ranges of $E < E_F$. If there are surface states in the gaps below E_F they should be occupied and detectable by photoemission experiments.[3,4] We have therefore performed eigenvalue calculations on thin (111) aluminum films using a method[5] which allows the potential to fall off outside the film in a continuous way. At the high-symmetry points we find surface states occupying all gaps. This result differs slightly from that of Boudreaux[6] who reported surface states at and around $\bar{\Gamma}$, the center of the 2D BZ, but none at $\bar{K}$ or $\bar{M}$. Our results are also interesting in that at $\bar{K}$ we find eigenstates in which the wave function is localized entirely on one face or the other of the film. All other surface eigenstates seen in this and preceding work[1,2,5] have had large amplitudes on both surfaces of the film. Only in the limit of an infinitely thick film would even and odd surface eigenstates become degenerate so that one could combine them to form eigenstates localized on one surface or the other.

A semi-infinite (111) aluminum crystal may be produced by slicing an infinite crystal perpendicular to the [111] crystal axis. Since aluminum has face-centered-cubic structure, this produces layers parallel to the surface in which the atoms are arranged with hexagonal symmetry. There are three types of layers and they repeat in an $ABCABC\cdots$ order along the [111] direction. For a thin film with an odd number of layers, this ordering implies inversion symmetry through one of the atoms in the central layer. For an even number of layers the inversion center lies at a point midway between the two central layers and directly below an atom of the third type of layer. In this respect the (111) film is different from the (001) and (110) films where, for an odd number of layers, there is reflection symmetry through the center of the film and for an even number of layers, a glide plane. Figure 1 shows the (111) crystal structure. The planar lattice vectors $\vec{a}$ and $\vec{b}$ are of length $a/\sqrt{2}$, where $a = 4.04$ Å is the edge length of the aluminum face-centered cube. The dashed lines indicate the sides of the planar unit cell. The unit cell for a film will have these planar dimensions times the thickness of the film, including a selvage region in which the potential and charge density fall to zero. The number of atoms in the unit cell will equal the number of occupied layers. The distance between successive layers is $a/\sqrt{3}$. Layers are farther apart in (111) films than in (001) or (110),

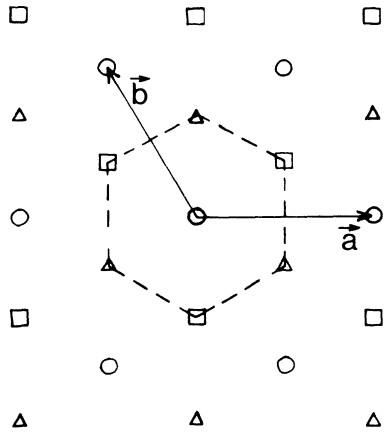

FIG. 1. Crystal structure of the (111) face of face-centered-cubic aluminum. Circles denote atoms in A layers; squares denote atoms in B layers; triangles denote atoms in C layers.

so that the (111) is the most densely packed face of the fcc crystal.

In Fig. 2(a) we show the relationship between

$$\vec{a} = \tfrac{1}{2}a(-1, 0, 1)\,, \quad \vec{b} = \tfrac{1}{2}a(1, -1, 0) \tag{1}$$

and their two-dimensional reciprocal-lattice vectors

$$\vec{K}_1 = (2\pi/a)(-\tfrac{2}{3}, -\tfrac{2}{3}, \tfrac{4}{3}), \quad \vec{K}_2 = (2\pi/a)(\tfrac{2}{3}, -\tfrac{4}{3}, \tfrac{2}{3})\,. \tag{2}$$

Figure 2(b) shows the 2D BZ. We adopt the notation for high-symmetry points which has previously been used for the surface-phonon problem.[7] In the hexagonal basis (2), $\bar{\Gamma} = (0, 0)$, $\bar{M} = (\frac{1}{2}, 0)$, and $\bar{K} = (\frac{1}{3}, \frac{1}{3})$. For comparison, the dashed line in Fig. 2(b) shows the $(\frac{1}{2}\frac{1}{2}\frac{1}{2})$ face of the 3D fcc BZ.

As explained in Refs. 1 and 2 (hereafter called I and II, respectively), the main features of the 2D energy bands can be found by projecting the 3D bands against the 2D BZ. This is most conveniently done by defining an extended-slab-adapted 3D BZ having the 2D BZ as base. The volume of the extended-slab-adapted BZ is the same as that of the usual 3D BZ, so that the two are equivalent. For the (111) face this means the slab-adapted BZ extends from $-\frac{1}{2}\vec{K}_3 < (2\pi/a)k_\zeta \leq \frac{1}{2}\vec{K}_3$, where

$$\vec{K}_3 = (2\pi/a)(1, 1, 1). \tag{3}$$

For an infinitely thick (111) film, the allowed eigenvalues at $\bar{\Gamma}$ are just allowed eigenvalues at the 3D points $(k_\zeta, k_\zeta, k_\zeta)$, for all $-\frac{1}{2} < k_\zeta \leq \frac{1}{2}$. We calculate the 3D eigenvalues from the same superposition of Heine-Animalu[8] pseudopotentials as in I and

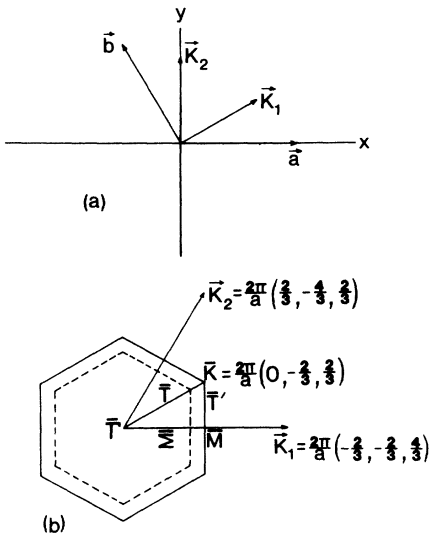

FIG. 2. (a) Relationship between the rectangular axes (x, y), the crystal lattice vectors $(\vec{a}, \vec{b})$ and the reciprocal-lattice vectors $(\vec{K}_1, \vec{K}_2)$, (b) The two-dimensional BZ for the (111) face of fcc aluminum. Equivalent directions in the 3D crystal are indicated.

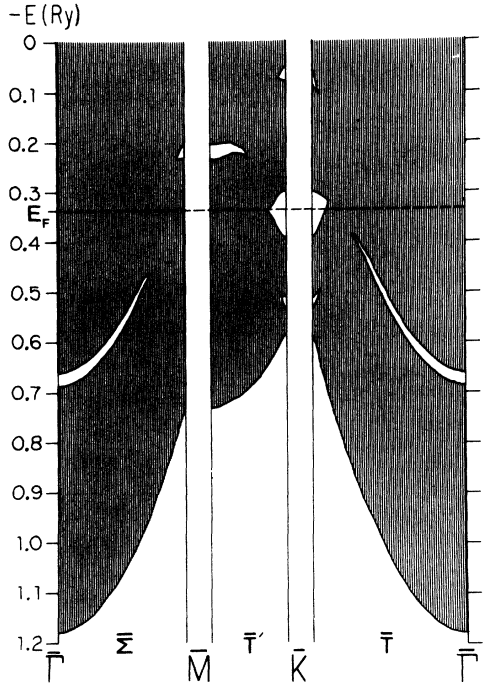

FIG. 3. Projected 2D energy bands derived from the 3D band structure.

II. Because we have inversion rather than reflection symmetry in the central plane, there is, for a general $\bar{k}$, no operation which leaves $\bar{k}$ unchanged while taking k_ζ to $-k_\zeta$. Therefore unlike the (001) and (110) films, eigenvalues for $\pm k_\zeta$ are not generally equal.

Figure 3 shows the main features of the 2D projection of the 3D bands. Since we are looking for surface states, which can exist only within band gaps, we use crosshatching to show a continuum of states, and show the band gaps. At $\bar{\Gamma}$ the gap comes from a repulsion between $k_\zeta = 0.5$ states. In 3D this is just the L point, $(\frac{1}{2}, \frac{1}{2}, \frac{1}{2})$. The inversion operation takes $\bar{\Gamma}$ into itself making all $\bar{\Gamma}$ eigenvalues twofold degenerate between $+k_\zeta$ and $-k_\zeta$ states (except at $k_\zeta = 0.5$).[9] This gap extends not only along both the $\bar{\Sigma}$ and $\bar{T}$ symmetry directions but in every direction between $k_\zeta = 0.5$ states which we have verified by calculating eigenvalues at a point of no symmetry about halfway between $\bar{\Gamma}$ and the middle of the $\bar{T}'$ line.

As we move from $\bar{\Gamma}$ toward $\bar{M}$ along the $\bar{\Sigma}$ line, we calculate 3D eigenvalues at $(k_\zeta - \frac{2}{3}\alpha,\ k_\zeta - \frac{2}{3}\alpha,\ k_\zeta + \frac{4}{3}\alpha)$, $0 \leq \alpha \leq \frac{1}{2}$, and $-\frac{1}{2} \leq k_\zeta < \frac{1}{2}$. The degeneracy between $+k_\zeta$ and $-k_\zeta$ is lost, and the lines diverge more the higher in energy they are. About 70% of the distance from $\bar{\Gamma}$ to $\bar{M}$ the $k_\zeta = -0.5$ gap is crossed by states with k_ζ approximately equal to 0.4 and disappears. At $\bar{M}$ there is a gap between

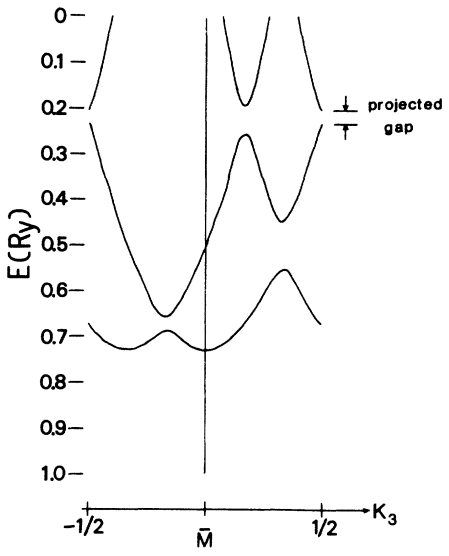

FIG. 4. 3D energy bands from $\bar{M}-\frac{1}{2}\vec{K}_3$ to $\bar{M}+\frac{1}{2}\vec{K}_3$. These are projected against $\bar{M}$ to make the 2D bands at $\bar{M}$.

$k_\zeta = 0.5$ states above E_F. This comes from the 3D point $\bar{M} \pm (2\pi/a)(\frac{1}{2}, \frac{1}{2}, \frac{1}{2}) = (2\pi/a)[(-\frac{1}{3}, -\frac{1}{3}, \frac{2}{3}) \pm (\frac{1}{2}, \frac{1}{2}, \frac{1}{2})]$ $= (2\pi/a)(\frac{1}{6}, \frac{1}{6}, \frac{7}{6})$ or $(2\pi/a)(-\frac{5}{6}, -\frac{5}{6}, \frac{1}{6})$, which becomes after subtracting a reciprocal-lattice vector, $(2\pi/a)(\frac{1}{6}, \frac{1}{6}, -\frac{5}{6})$. In Fig. 4 we show the 3D energy bands along a line from $\bar{M} - (2\pi/a)(\frac{1}{2}, \frac{1}{2}, \frac{1}{2})$ to $\bar{M}$ $+(2\pi/a)(\frac{1}{2}, \frac{1}{2}, \frac{1}{2})$. We note that there is a second gap in the 3D bands at about $k_\zeta = \frac{1}{6}$ not much wider than the projected gap so that surface states in the $\bar{M}$ gap are not expected to fall off like a single exponential. The $\bar{M}$ gap pinches off in the $\bar{\Sigma}$ direction as the $k_\zeta = 0.5$ lines are crossed by lines with k_ζ of approximately 0.2.

Along $\bar{T}'$ from $\bar{M}$ to $\bar{K}$ we calculate eigenvalues at the 3D points $(k_\zeta + \alpha - \frac{1}{3},\ k_\zeta - \alpha - \frac{1}{3},\ k_\zeta + \frac{2}{3})$, $0 \le \alpha \le \frac{1}{3}$ and $-\frac{1}{2} < k_\zeta \le \frac{1}{2}$. The $\bar{M}$ gap extends about $\frac{1}{3}$ of the way toward $\bar{K}$ as a gap between $k_\zeta = 0.5$ states until it pinches off as states of other k_ζ cross the gap. At $\bar{K}$ there are three different gaps. The gap between -0.3 and -0.4 Ry is between $k_\zeta = 0$ states. The narrower gaps about -0.06 and -0.525 Ry come from $k_\zeta = 0.5$. All these gaps pinch off quickly along $\bar{T}'$. Note that since E_F $= -0.33$ Ry lies near the middle of one gap at $\bar{K}$, there is a possibility that a surface state might exist below E_F at $\bar{K}$ and cross the Fermi level as we go away from $\bar{K}$.

Along $\bar{T}$ we calculate eigenvalues at the 3D points $(k_\zeta, k_\zeta - \alpha, k_\zeta + \alpha)$, $0 \le \alpha \le \frac{2}{3}$ and $-\frac{1}{2} < k_\zeta \le \frac{1}{2}$. Along this direction all states are twofold degenerate between $+k_\zeta$ and $-k_\zeta$. The two are related by a twofold rotation about the $[0\bar{1}1]$ axis, a 3D symmetry operation. Between $\bar{K}$ and $\bar{\Gamma}$, all the $\bar{K}$ gaps are pinched off quickly. As indicated above, the gap at $\bar{\Gamma}$ extends 75% of the way toward $\bar{K}$. The gap pinches off as the two $k_\zeta = 0.5$ states become degenerate at the 3D W point, i.e., $\frac{3}{4}\bar{K} + (2\pi/a)(\frac{1}{2}, \frac{1}{2}, \frac{1}{2}) = (2\pi/a)$ $\times[(0, -\frac{1}{2}, \frac{1}{2}) + (\frac{1}{2}, \frac{1}{2}, \frac{1}{2})] = (2\pi/a)(\frac{1}{2}, 0, 1)$.

In order to do an eigenvalue calculation, we have generated thin-film potentials from overlapping aluminum[8] pseudopotentials. The Lang-Kohn jellium potential[10] has been incorporated into the $\bar{G} = 0$ Fourier transform of the thin-film potential as in I and II in order to improve the falloff outside the film. This is shown in Fig. 5. This figure also shows that the planar average of the pseudopotential rises to a peak midway between layers of atoms. This results from our use of a pseudopotential which has its minimum closer to the atom than one-half the (111) interplanar spacing. This effect was not seen in the $\bar{G} = 0$ transforms of the (110) and (001) potentials where the layers are closer together.

The basis functions in which we expand the wave functions are the same as those used previously.[1,2,5] Plane waves are used to expand the planar part of the wave function, and the part of the wave function in the [111] direction is expanded in sines and cosines of $k_z z$ ($k_z \equiv k_\zeta 2\pi/a$.) Values of k_ζ are chosen so that the wave function is identically zero at the outer edge of the selvage region.[5] In previous work, reflection symmetry through the center layer of the film has implied that each irreducible representation would contain only sines or cosines of

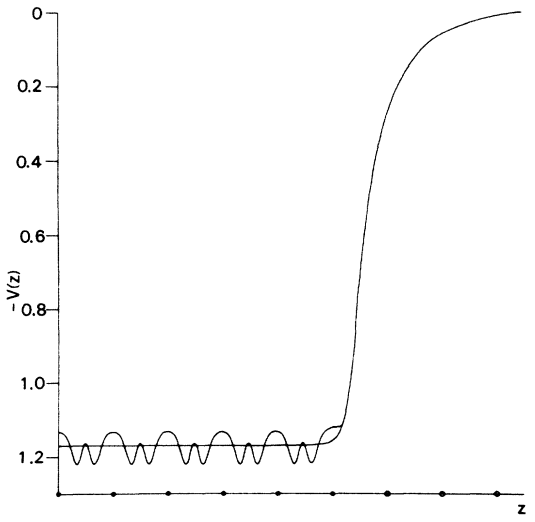

FIG. 5. $\bar{G} = 0$ Fourier transform of the potential for a (111) aluminum film of 11 occupied layers and three selvage layers on each side. The potential is shown for $z > 0$, and the jellium edge is halfway between the last occupied and the first unoccupied layer. The potential for jellium of the appropriate electron density is also shown.

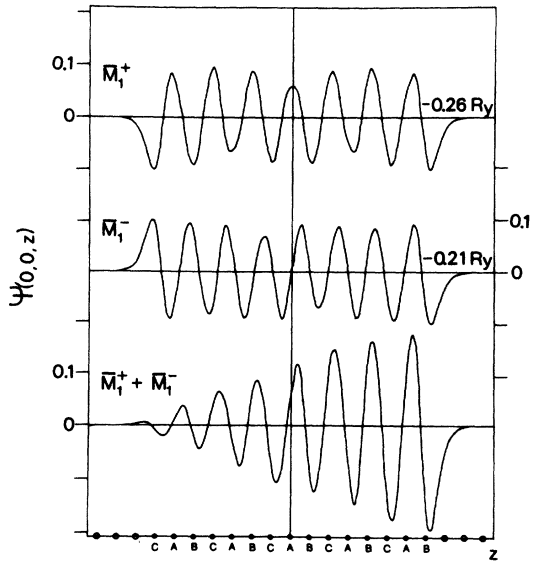

FIG. 6. $\bar{M}_1^+$ and $\bar{M}_1^-$ surface states, and the sum of these two wave functions. Results are shown for a film of 15 occupied layers and three selvage layers on each side. Layers are labeled and eigenvalues given.

$k_z z$. Here both sines and cosines will appear in each irreducible representation. But because of the inversion symmetry, the total number of basis functions will be about the same.[11] We expect that, at $\bar{\Gamma}$, three planar-symmetrized combinations of plane waves (S2DPW) will be needed for planar convergence. For the potential in Fig. 5, we expect thirty values of sines and cosines to be needed for convergence in the z direction. We have tested the convergence at $\bar{\Gamma}$ from three S2DPWs and thirty values of $\sin(k_z z)$ and $\cos(k_z z)$. For three S2DPWs and sixty sines and cosines, no eigenvalue changes by more than 0.0012 Ry. For six S2DPWs and thirty sines and cosines, no eigenvalue changes by more than 0.0032 Ry. Using these convergence criteria we project the number of S2DPWs, sines and cosines needed for convergence at other $\vec{k}$ points and for other film thicknesses.

We have calculated eigenvalues and eigenfunctions at the $\bar{\Gamma}$, $\bar{M}$, and $\bar{K}$ points. We have used the thickest films which give us eigenvalue matrices no larger than 280×280. This makes it easier to see the exponential falloff of the surface states. We can make the falloff still clearer by calculating the wave functions across the full thickness of the films. Wave functions which are even and odd with respect to inversion can be added and subtracted to show states localized on one surface of the film or the other. These results will not be exact, since the states of even and odd symmetry are not exactly degenerate. The thinner the film is, the more the degeneracy is split. But even the worst case, shown in Fig. 6, is not bad. For the $\bar{M}$ point we need seven S2DPWs for planar convergence, and can only work with a film of fifteen occupied layers and three selvage layers on each side. The eigenvalues for the surface states are −0.259 Ry for $\bar{M}_1^+$ and −0.212 Ry for $\bar{M}_1^-$. Figure 6 shows the $\bar{M}_1^+$ and $\bar{M}_1^-$ surface states plotted for the full width of the film, at $\bar{r}=(0,0)$ a point through which inversion symmetry just takes $(\bar{r}, z)$ into $(\bar{r}, -z)$.[12] For this value of $\bar{r}$ the wave function goes through atoms in the A planes. This makes the peaks in the wave functions especially small near A planes and obscures the exponential falloff of the wave functions, especially for $\bar{M}_1^+$. We therefore also plot the sum of the $\bar{M}_1^+$ and $\bar{M}_1^-$ wave functions. The difference between the two wave functions is just the mirror image of the sum.

The surface states in the center gap at $\bar{K}$ belong to the two-dimensional irreducible representation $\bar{K}_2$ and are twofold degenerate. Neither partner of this representation is either even or odd with respect to all the operations of the $\bar{K}$ group which take z into $-z$. The eigenfunctions need not be even or odd with respect to the center of the film, and can be localized entirely on one face of the film if we choose our S2DPW correctly. Figure 7 shows the $\bar{K}_2$ state localized on the left face of a thirteen layer film. This surface state has eigenvalue −0.379 Ry and lies below the Fermi level. Since the gap in which this state lies extends to above the Fermi level in the $\bar{T}$ direction, it is probable that the (111) crystal surface will have a Fermi line such as we have previously discussed[2] for the (110) surface.

The $\bar{\Gamma}$ gap is occupied by $\bar{\Gamma}_1^+$ surface states, while the upper and lower $\bar{K}$ gaps are occupied by $\bar{K}_1^+$ surface states. For both $\bar{\Gamma}_1^+$ and $\bar{K}_1^+$ we can work with a film of 33 occupied layers. For this film thickness, the $\bar{\Gamma}_1^+$ and $\bar{\Gamma}_1^-$ eigenvalues are −0.683 and −0.666 Ry, respectively. The $\bar{K}_1^+$ eigenvalues are −0.526 and −0.078 Ry. The $\bar{K}_1^-$ eigenvalues are

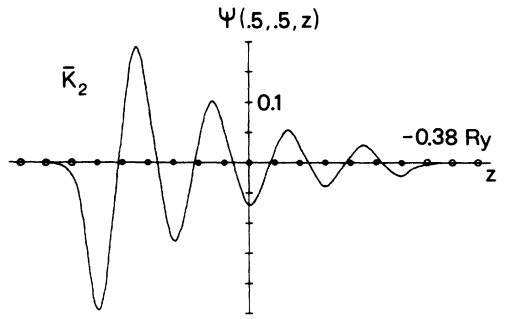

FIG. 7. $\bar{K}_2$ surface state and its eigenvalue. Results are shown for a film of 13 occupied layers and three selvage layers on each side.

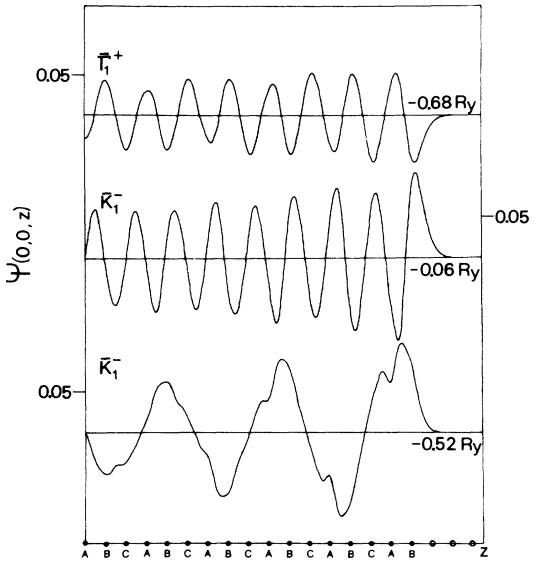

FIG. 8. $\bar{\Gamma}_1^+$ and $\bar{K}_1^-$ surface states and their eigenvalues. Results are shown for the right-half of a film of 33 occupied layers, which are labeled. There are three selvage layers on each side of the film.

-0.522 and -0.064 Ry. Figure 8 shows the $\bar{\Gamma}_1^+$ and $\bar{K}_1^-$ surface states. The decay of the $\bar{\Gamma}_1^+$ state is small because of the narrowness of the $\bar{\Gamma}$ gap. Furthermore, the decay does not seem to be smooth. This is because the $\bar{\Gamma}_1^\pm$ surface states comes mainly from the three-dimensional L_1 states $\vec{k} = \pm(2\pi/a)(\frac{1}{2}, \frac{1}{2}, \frac{1}{2})$. Since z is in the (1, 1, 1) direction one sees that $k_z z$ changes by π over an interplanar spacing. Therefore a maximum or minimum occurs for each interplanar spacing. The crystal, however, is periodic over a distance of three (111) interplanar spacings and if one examines every third extremum of the $\bar{\Gamma}_1^+$ surface state one indeed sees that they decay reasonably smoothly. The same effect occurred for (001) and (110) films.[1,2] There the crystal periodicity was over two interplanar spacings so that the maxima decayed smoothly as did the minima, but if one looks at the maxima and minima together one sees that they do not decay smoothly.

We thus see that in the (111) face of aluminum all energy band gaps at high symmetry points are occupied by surface states. This also proved to be the case for the other two faces of aluminum which we have studied, and for the (001) face of Li. Where we have been able to calculate eigenvalues and eigenfunctions along lines between high-symmetry points we have seen that the surface states extend along the gaps until just before the gap cutoff. It is our conjecture that surface states exist in all gaps of any simple-metal low-index surface. This contradicts the claim of Gurman and Pendry[13]

TABLE I. Character table for the group at $\bar{\Gamma}$.

$\bar{\Gamma}$	E	$2C_3$	$3\sigma_v$	Π	$2\bar{C}_3$	$3\bar{\sigma}_v$
$\bar{\Gamma}_1^+$	1	1	1	1	1	1
$\bar{\Gamma}_1^-$	1	1	1	−1	−1	−1
$\bar{\Gamma}_2^+$	1	1	−1	1	1	−1
$\bar{\Gamma}_2^-$	1	1	−1	−1	−1	1
$\bar{\Gamma}_3^+$	2	−1	0	2	−1	0
$\bar{\Gamma}_3^-$	2	−1	0	−2	1	0

that for gaps at the 3D BZ boundary, the existence of a surface state depends on the sign of the matrix element responsible for the gap and therefore there is only a 50% chance of a surface state at the zone boundary. This result has been shown by one of us[14] to be true only when the matrix element $V(\vec{k})$ has $\vec{k}$ along the surface normal. For a model consisting of weak $V(\vec{k})e^{i\vec{k}\cdot\vec{r}}$ potentials superposed inside a finite square-well potential, he has shown a surface state always exists if there are a pair of degenerate $V(\vec{k}_i)$ and $V(\vec{k}_j)$ such that $\vec{k}_i + \vec{k}_j$ lies along the surface normal. It seems likely that in a real metal there are a sufficient number of $V(\vec{k})$ present that one can always satisfy this condition for low-index surfaces. The effect of having a smooth potential rather than the discontinuous model potential is not completely clear. However, the fact that the model potential result is independent of where one chooses to put the discontinuity leads us to believe that the result holds for a realistic continuous potential.

In this paper, as in our previous work on other faces of aluminum, we have found surface states which were not found by Boudreaux[6] in calculations with a discontinuous potential. It is clear that there should be effects of this difference in potentials, e.g., on the decay constants of the surface states. But considering the results of our calculation[14] with discontinuous potentials, it does not seem that this difference in potentials can cause the disappearance of the surface states.

APPENDIX: GROUP THEORY

For a (111) film with either an odd or even number of layers, there is inversion symmetry through a point in the central plane. The group for this film is just the triangle group—$C_{3v}(3m)$—times the

TABLE II. Character table for the group at $\bar{M}$.

$\bar{M}$	E	σ_1	Π	$\bar{\sigma}_1$
$\bar{M}_1^+$	1	1	1	1
$\bar{M}_1^-$	1	1	−1	−1
$\bar{M}_2^+$	1	−1	1	−1
$\bar{M}_2^-$	1	−1	−1	1

TABLE III. Character table for the group at $\bar{K}$.

$\bar{K}$	E	C_3	C_3^2	$\bar{\sigma}_1$	$\bar{\sigma}_2$	$\bar{\sigma}_3$
$\bar{K}_1^+$	1	1	1	1	1	1
$\bar{K}_1^-$	1	1	1	−1	−1	−1
$\bar{K}_2$	$\begin{pmatrix} 1 & 0 \\ 0 & 1 \end{pmatrix}$	$\begin{pmatrix} -\frac{1}{2} & \frac{1}{2}\sqrt{3} \\ \frac{1}{2}\sqrt{3} & -\frac{1}{2} \end{pmatrix}$	$\begin{pmatrix} -\frac{1}{2} & -\frac{1}{2}\sqrt{3} \\ \frac{1}{2}\sqrt{3} & -\frac{1}{2} \end{pmatrix}$	$\begin{pmatrix} 1 & 0 \\ 0 & -1 \end{pmatrix}$	$\begin{pmatrix} -\frac{1}{2} & \frac{1}{2}\sqrt{3} \\ \frac{1}{2}\sqrt{3} & \frac{1}{2} \end{pmatrix}$	$\begin{pmatrix} -\frac{1}{2} & -\frac{1}{2}\sqrt{3} \\ -\frac{1}{2}\sqrt{3} & \frac{1}{2} \end{pmatrix}$

inversion. The triangle group contains two threefold rotations and three reflection lines which bisect the angles at the vertices of the triangle. If we use Π to denote the inversion, and a bar over an operation to denote the operation multiplied by Π, then the group at $\bar{\Gamma}$ is just given by the character table shown in Table I.

At $\bar{M}$ we have only four operations, E, Π, σ_1, that σ_v plane in which $\bar{M}$ lies, and $\bar{\sigma}_1$. The character table is given in Table II.

At $\bar{K}$ there are six operations, E, $2C_3$, and $3\bar{\sigma}_v$, and the irreducible representations are given by Table III.

We list below the S2DPW for those irreducible representations which have negative energy, in terms of the nonorthogonal vectors $\vec{K}_1 = (2\pi/a) \times (-\frac{2}{3}, -\frac{2}{3}, \frac{4}{3})$ and $\vec{K}_2 = (2/a)(\frac{2}{3}, -\frac{4}{3}, \frac{2}{3})$. The $\bar{\Gamma}_1^-$, $\bar{M}_1^-$, $\bar{K}_1^-$, and $(\bar{K}_2)_2$ S2DPW are obtained by replacing $\sin(k_z z)$ and $\cos(k_z z)$ in $\bar{\Gamma}_1^+$, $\bar{M}_1^+$, $\bar{K}_1^+$ and $(\bar{K}_2)_1$ by $\cos(k_z z)$ and $\sin(k_z z)$.

$\bar{\Gamma}_1^+$: $\Psi_1 = |0, 0\rangle \cos(k_z z)$,

$\Psi_2 = (1/\sqrt{6})(|1, 0\rangle + |-1, 0\rangle + |0, -1\rangle + |0, 1\rangle + |-1, 1\rangle + |1, -1\rangle) \cos(k_z z)$,

$\Psi_3 = (1/\sqrt{6})(|1, 0\rangle - |-1, 0\rangle + |0, -1\rangle - |0, 1\rangle + |-1, 1\rangle - |1, -1\rangle) \sin(k_z z)$;

$\bar{M}_1^+$: $\Psi_1 = (1/\sqrt{2})(|\frac{1}{2}, 0\rangle + |-\frac{1}{2}, 0\rangle) \cos(k_z z)$,

$\Psi_2 = (1/\sqrt{2})(|\frac{1}{2}, 0\rangle - |-\frac{1}{2}, 0\rangle) \sin(k_z z)$,

$\Psi_3 = (1/\sqrt{2})(|\frac{3}{2}, 0\rangle + |-\frac{3}{2}, 0\rangle) \cos(k_z z)$,

$\Psi_4 = (1/\sqrt{2})(|\frac{3}{2}, 0\rangle - |-\frac{3}{2}, 0\rangle) \sin(k_z z)$,

$\Psi_5 = \frac{1}{2}(|\frac{1}{2}, 1\rangle + |\frac{3}{2}, -1\rangle + |-\frac{1}{2}, -1\rangle + |-\frac{3}{2}, 1\rangle) \cos(k_z z)$,

$\Psi_6 = \frac{1}{2}(|\frac{1}{2}, 1\rangle + |\frac{3}{2}, -1\rangle - |-\frac{1}{2}, -1\rangle - |-\frac{3}{2}, 1\rangle) \sin(k_z z)$,

$\Psi_7 = (1/\sqrt{2})(|\frac{1}{2}, -1\rangle + |-\frac{1}{2}, 1\rangle) \cos(k_z z)$;

$\bar{K}_1^+$: $\Psi_1 = (1/\sqrt{3})(|\frac{1}{3}, \frac{1}{3}\rangle + |\frac{1}{3}, -\frac{2}{3}\rangle + |-\frac{2}{3}, \frac{1}{3}\rangle) \cos(k_z z)$,

$\Psi_2 = (1/\sqrt{6})(|\frac{4}{3}, \frac{1}{3}\rangle + |\frac{1}{3}, -\frac{5}{3}\rangle + |-\frac{5}{3}, \frac{4}{3}\rangle + |-\frac{5}{3}, \frac{1}{3}\rangle + |\frac{4}{3}, -\frac{5}{3}\rangle + |\frac{1}{3}, \frac{4}{3}\rangle) \cos(k_z z)$,

$\Psi_3 = (1/\sqrt{6})(|\frac{4}{3}, \frac{1}{3}\rangle + |\frac{1}{3}, -\frac{5}{3}\rangle + |-\frac{5}{3}, \frac{4}{3}\rangle - |-\frac{5}{3}, \frac{1}{3}\rangle - |\frac{4}{3}, -\frac{5}{3}\rangle - |\frac{1}{3}, \frac{4}{3}\rangle) \sin(k_z z)$,

$\Psi_4 = (1/\sqrt{3})(|-\frac{2}{3}, \frac{4}{3}\rangle + |\frac{4}{3}, -\frac{2}{3}\rangle + |-\frac{2}{3}, -\frac{2}{3}\rangle) \cos(k_z z)$;

$(\bar{K}_2)_1$: $\Psi_1 = (\sqrt{\frac{2}{3}})(\frac{1}{2}|\frac{1}{3}, \frac{1}{3}\rangle - |\frac{1}{3}, -\frac{2}{3}\rangle + \frac{1}{2}|-\frac{2}{3}, \frac{1}{3}\rangle) \cos(k_z z)$,

$\Psi_2 = (1/\sqrt{2})(|\frac{1}{3}, \frac{1}{3}\rangle - |-\frac{2}{3}, \frac{1}{3}\rangle) \sin(k_z z)$,

$\Psi_3 = (\sqrt{\frac{2}{3}})(\frac{1}{2}|-\frac{2}{3}, -\frac{2}{3}\rangle - |-\frac{2}{3}, \frac{4}{3}\rangle + \frac{1}{2}|\frac{4}{3}, -\frac{2}{3}\rangle) \cos(k_z z)$,

$\Psi_4 = (1/\sqrt{2})(|-\frac{2}{3}, -\frac{2}{3}\rangle - |\frac{4}{3}, -\frac{2}{3}\rangle) \sin(k_z z)$,

$\Psi_5 = (1/\sqrt{3})(|\frac{4}{3}, \frac{1}{3}\rangle - \frac{1}{2}|\frac{1}{3}, -\frac{5}{3}\rangle - \frac{1}{2}|-\frac{5}{3}, \frac{4}{3}\rangle + |-\frac{5}{3}, \frac{1}{3}\rangle - \frac{1}{2}|\frac{4}{3}, -\frac{5}{3}\rangle - \frac{1}{2}|\frac{1}{3}, \frac{4}{3}\rangle) \cos(k_z z)$,

$\Psi_6 = (1/\sqrt{3})(|\frac{4}{3}, \frac{1}{3}\rangle - \frac{1}{2}|\frac{1}{3}, -\frac{5}{3}\rangle - \frac{1}{2}|-\frac{5}{3}, \frac{4}{3}\rangle - |-\frac{5}{3}, \frac{1}{3}\rangle + \frac{1}{2}|\frac{4}{3}, -\frac{5}{3}\rangle + \frac{1}{2}|\frac{1}{3}, \frac{4}{3}\rangle) \sin(k_z z)$,

$\Psi_7 = \frac{1}{2}(|\frac{1}{3}, -\frac{5}{3}\rangle - |-\frac{5}{3}, \frac{4}{3}\rangle + |\frac{4}{3}, -\frac{5}{3}\rangle - |\frac{1}{3}, \frac{4}{3}\rangle) \cos(k_z z)$,

$\Psi_8 = \frac{1}{2}(|\frac{1}{3}, -\frac{5}{3}\rangle - |-\frac{5}{3}, \frac{4}{3}\rangle - |\frac{4}{3}, -\frac{5}{3}\rangle + |\frac{1}{3}, \frac{4}{3}\rangle) \sin(k_z z)$.

Note that the $\bar{K}_2$ surface states which are large on only one of the two surfaces of the film transform according to $(\bar{K}_2)'_{1,2} = 2^{-1/2}[(\bar{K}_2)_1 \pm (\bar{K}_2)_2]$.

---

*Research supported by the Air Force Office of Scientific Research under Grant No. AF-AFOSR-72-2308 and by the National Science Foundation under Grant No. GH-40371.

[1]E. B. Caruthers, L. Kleinman and G. P. Alldredge, Phys. Rev. B 8, 4570 (1973).

[2]E. B. Caruthers, L. Kleinman and G. P. Alldredge, preceding paper, Phys. Rev. B 9, 3325 (1974).

[3]B. J. Waclawski and E. W. Plummer, Phys. Rev. Lett. 29, 783 (1972).

[4]B. Feuerbacher and B. Fitten, Phys. Rev. Lett. 29, 786 (1972).

[5]G. P. Alldredge and L. Kleinman, Phys. Rev. Lett. 28, 1264 (1972).

[6]D. S. Boudreaux, Surf. Sci. 28, 344 (1971).

[7]R. E. Allen, G. P. Alldredge, and F. W. de Wette, Phys. Rev. B 4, 1661 (1971).

[8]A. O. E. Animalu and V. Heine, Philos. Mag. 12, 1249 (1965).

[9]$k_\zeta = 0.5$ and $k_\zeta = -0.5$ are separated by the reciprocal-lattice vector (1, 1, 1) and are not independent.

[10]N. D. Lang and W. Kohn, Phys. Rev. B 1, 4555 (1970).

[11]Each S2DPW is multiplied by either a $\sin(k_z z)$ or a $\cos(k_z z)$ but not both, though the same PWs may appear in one S2DPW multiplied by $\sin(k_z z)$ and in another S2DPW multiplied by $\cos(k_z z)$. For example, a representation even under the inversion will contain odd S2DPW times $\sin(k_z z)$ and even S2DPW times $\cos(k_z z)$.

[12]If one chooses an $\bar{\mathbf{r}}$ other than (00), $(\frac{1}{2}\frac{1}{2})$, $(\frac{1}{2}0)$, or $(0\frac{1}{2})$ the inversion takes $(\bar{\mathbf{r}}, z)$ into $(-\bar{\mathbf{r}}, -z)$ and the plot of the wave function for fixed $\bar{\mathbf{r}}$ is not purely even or odd under $z \to -z$. However because a surface eigenstate decays inwardly from the surfaces at both $\bar{\mathbf{r}}$ and $-\bar{\mathbf{r}}$, the sum and difference of even and odd (under inversion) surface eigenstates will be surface states localized on one or the other of the thin-film surfaces.

[13]S. J. Gurman and J. B. Pendry, Phys. Rev. Lett. 31, 637 (1973).

[14]L. Kleinman, Phys. Rev. B 6, 1142 (1972).

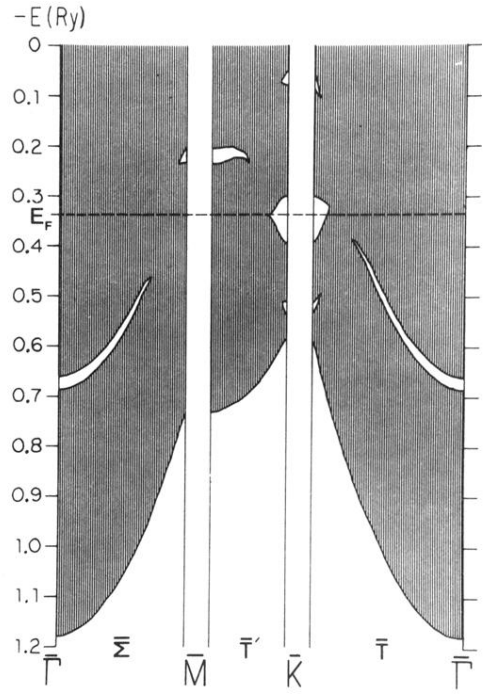

FIG. 3. Projected 2D energy bands derived from the 3D band structure.